



Title	Photoelectrochemical and Photoluminescence (PL) Properties of p-Type Porous Silicon/Electrolyte Solution Interface : Potential Dependent PL Spectra as a Result of Size Dependent Quenching
Author(s)	Noguchi, Hidenori; Kondo, Toshihiro; Uosaki, Kohei
Citation	Journal of Physical Chemistry B, 101(25), 4978-4981 https://doi.org/10.1021/jp970309d
Issue Date	1997-06-19
Doc URL	http://hdl.handle.net/2115/50248
Type	article
File Information	JPCB101-25_4978-4981.pdf



[Instructions for use](#)

Photoelectrochemical and Photoluminescence (PL) Properties of p-Type Porous Silicon/Electrolyte Solution Interface: Potential Dependent PL Spectra as a Result of Size Dependent Quenching

Hidenori Noguchi, Toshihiro Kondo, and Kohei Uosaki*

Physical Chemistry Laboratory, Division of Chemistry, Graduate School of Science, Hokkaido University, Sapporo 060, Japan

Received: January 23, 1997[⊗]

Potential dependences of the photocurrent and visible photoluminescence (PL) from p-type porous silicon (p-PS) in 0.2 M Na₂SO₄ aqueous solution were investigated. When the potential became more negative than -0.6 V, a cathodic photocurrent was observed and PL was quenched. When the potential was swept back in the positive direction, the PL intensity increased, the photocurrent decreased, and both returned to the initial values. PL spectra measurements showed that the quenching of the PL intensity was accompanied by a blue shift of the peak wavelength as a result of the selective quenching of the red portion of the PL spectra. The experimentally observed results can be explained by considering the dependence of electron accumulation on the conduction band levels in PS layer, which is in turn related to the Si nanocrystalline size.

Introduction

Since the recent discovery of visible light emission from porous silicon (PS),¹ many researches on PS have been carried out by many research groups because of the possible development of Si-based optoelectronic devices.² The electronic properties of bulk silicon cannot explain the above phenomenon as silicon has the indirect band gap of 1.1 eV. One explanation for the visible luminescence is based on the nanometer-size crystalline structure for PS.³ This structure can exploit quantum confinement effects which are responsible for band gap widening into the visible range.^{3,4} The contribution of chemical species such as siloxene (Si₆O₃H₆) to the luminescence has also been pointed out.⁵

The luminescence properties of the semiconductor/electrolyte solution interface are known to provide useful information of the mechanism of electrochemical reactions as well as the potential distribution at the interface.⁶ Electroluminescence (EL) is generated under forward bias by a radiative recombination of injected minority carriers with majority carriers, and its measurement is used to probe the reaction intermediates and the surface states of semiconductor electrodes.⁷ PS also shows EL in solution similar to ordinary semiconductor electrodes.^{8,9} For example, when a negative potential was applied to an n-PS electrode in a solution containing a hole injector such as S₂O₈²⁻, visible EL was observed.⁸ On the other hand, EL was reported at p-PS when it was anodically polarized in a solution containing only supporting electrolyte.^{9,10} We have investigated the relations between the chemical nature of PS and the EL properties of PS by XPS¹¹ and FT-IR measurements¹⁰ and demonstrated that the hydrogenated surface of p-PS acts as the required electron source for EL from the p-PS/electrolyte solution interface.

Interest in PS has been stimulated by the discovery of voltage-induced wavelength tuning of EL and photoluminescence (PL).^{12,13} PL measurements are often used to determine the quantum efficiency of photoelectrochemical reactions and to probe potential distributions across semiconductor electrode/

electrolyte solution interfaces.¹⁴ Thus, one can expect that PL measurements of PS/electrolyte solution interfaces provide useful information on the nature of PS. Only few reports on PL of PS/electrolyte solution interfaces are available, and they are on n-PS in the forward bias condition.^{12,13}

In this paper, we report the effect of a bias voltage on the photocurrent and the visible PL characteristics at a p-PS/electrolyte solution interface. When the potential became more negative than ca. -0.6 V, a cathodic photocurrent started to flow and PL was quenched accompanied by a blue shift of the peak wavelength.

Experimental Section

Preparation of Porous Silicon. Silicon wafers used in these experiments were p-type (8–12 Ω cm) single crystals obtained from Shin-Etsu Semiconductor with a (100) surface. The wafers were cleaned first with acetone to remove organic impurities and then with pure water and then chemically etched in 10% HF-ethanol solution for 1 min. The resulting thickness of the PS layer was approximately 670 nm. After ohmic contact was obtained by In-Zn alloy, the sample was placed in an electrode holder made from Teflon so that only one face of the wafer was exposed (apparent exposed area, 0.283 cm²). Constant current anodic oxidation was carried out in 10% HF-ethanol solution by using a potentiostat/galvanostat (Hokuto Denko, HA-151) in a Teflon cell with a Pt wire as a counter electrode. Current density for the porous formation was 5 mA/cm², and oxidation time was 600 s. The as-prepared p-PS was rinsed with a purified water and transferred to the spectroelectrochemical cell without exposure to air before the photoelectrochemical and the PL measurements to prevent dryness¹⁵ as well as native oxide growth.¹⁶

Photoelectrochemical and Photoluminescence Measurements. Photoelectrochemical measurements were carried out in 0.2 M Na₂SO₄ aqueous solution in a three-electrode glass cell which has an optical window. Ag/AgCl (saturated KCl) and a Pt wire were employed as a reference electrode and a counter electrode, respectively. The electrolyte solution was prepared using reagent grade Na₂SO₄ and Milli-Q water and deaerated by passing high-purity nitrogen gas (99.99%) through it prior to the photoelectrochemical and the PL measurements.

* To whom correspondence should be addressed. E-mail: uosaki@PCL.chem.hokudai.ac.jp.

[⊗] Abstract published in *Advance ACS Abstracts*, June 1, 1997.

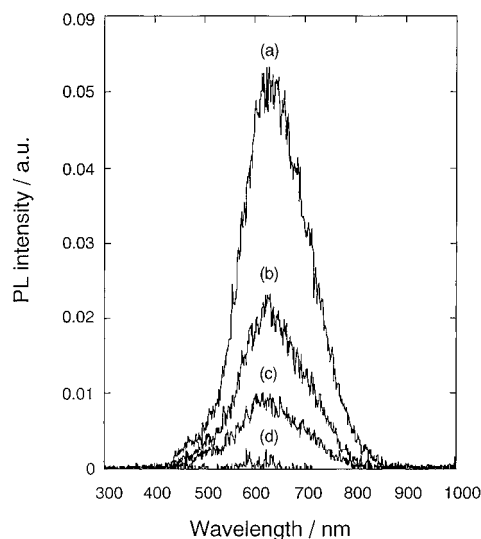


Figure 1. PL spectra of p-PS observed at various excitation intensities in 0.2 M Na_2SO_4 at -0.5 V with the excitation wavelength of 360 nm. The relative excitation intensities were (a) 100, (b) 53, (c) 30, and (d) 4.

Potential was controlled by using a potentiostat/galvanostat (Toho Technical Research, 2001) and a function generator (Hokuto Denko, HB-111). A monochromatic UV light (from 300 to 410 nm) from a 500 W Xe lamp (Ushio Electric. Co. Ltd., UXL-500D-O) was employed as an excitation light source. The excitation light intensity was kept constant by adjusting the lamp current to avoid the possible effect of excitation light intensity on the PL property. PL intensity was measured by using a photomultiplier tube (PMT: Hamamatsu Photonics Co. Ltd., R928). A long pass filter (Toshiba Glass Co. Ltd., Y-44), which allows transmission only above 410 nm, was used in order to eliminate the excitation light. The current and PMT output signals were recorded by using a personal computer (NEC Corp., PC-9801RA) through a 12 bit AD converter. PL spectra were obtained by using a multichannel detector (plasma coupled device: PCD) with an image intensifier (Hamamatsu Photonics Co. Ltd., IMD-C3300) combined with an imaging spectrograph (Jobin Yvon, CP-200; $f = 2.9$). The PCD elements were cooled to -20 °C. The exposure time was 3 s, and signals were obtained without averaging the PCD response. The optical system is sensitive from 1.4 to 3.4 eV with a resolution of 4 nm. All measurements were carried out at room temperature.

Results and Discussion

PL from p-Type PS/Electrolyte Solution Interface. Figure 1 shows the typical PL spectra from p-PS/electrolyte solution interface under various excitation light intensities measured in 0.2 M Na_2SO_4 . In this experiment the exposure time for the PCD system was 100 ms and the signal was averaged over 10 exposures. The potential was kept constant at -0.5 V during the spectral measurements, and the excitation light wavelength was 360 nm. The incident light was passed through several neutral density filters (Toshiba Glass Co. Ltd., ND-25, 50, and 70) to adjust the excitation intensity. The peak wavelength was ca. 660 nm, and the full width at half-maximum (fwhm) of the PL spectra was ca. 0.48 eV. The change in the excitation light intensity did not affect the shape of the PL spectra but affected the PL intensity. Although PL spectra from the PS/electrolyte solution interface were reported by Bsiesy et al.¹² and Meulenkamp et al.¹³ on n-PS in 1.0 M H_2SO_4 solution, the peak wavelength was ca. 700 nm. The difference in the PL peak

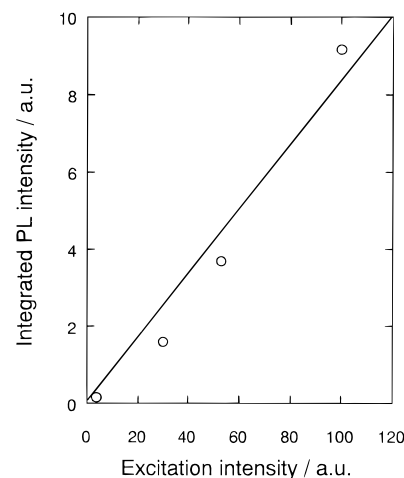


Figure 2. The relation between the integrated PL intensity and the excitation intensity. The integrated PL intensity was obtained by the integration of the PL spectra in Figure 1 from 300 to 1.000 nm.

wavelength between our results and those previously reported^{12,13} might be related to the significantly different microstructures of p-PS and n-PS.¹⁷

Figure 2 shows the relation between the integrated PL intensity and the excitation light intensity. It is clear that the integrated PL intensity increases in proportion to the excitation light intensity in the range of the present experiment. This result implies that PL from the p-PS/electrolyte solution interface is observed as a result of recombination of photogenerated electron-hole pairs.

Potential and Excitation Light Wavelength Dependence of PL Spectra. Figure 3 shows the PL spectra at various potentials recorded during the potential sweep between 0 and -1.2 V with a sweep rate of 20 mV/s under monochromatic 330, 360, and 390 nm light excitation in 0.2 M Na_2SO_4 aqueous solution. As the excitation light wavelength became longer, the intensity of the emitted light from the p-PS became smaller. When the potential was swept in the negative direction, a quenching of the PL intensity accompanied by a blue shift of the peak wavelength was observed as a result of the selective quenching of the red portion (low energy) of the spectra. No potential dependence was observed, however, for the blue portion (high energy) of the PL spectra. When the potential was swept back in the positive direction, the red portion of the PL spectra gradually recovered. The electrically induced quenching of the PL intensity from PS was also reported by Bsiesy et al.¹² and Meulenkamp et al.¹³ on n-PS in forward bias condition. Although they demonstrated that the visible PL from an n-PS/electrolyte solution interface is reversibly quenched by negative biases due to the quenching of the red portion (low energy) of the PL spectra, little attention has been given to the dependence of excitation light wavelength on voltage tuning of the PL spectra.

The quenching of the red portion increased quite significantly as the excitation light wavelength became longer.

Current–Potential and PL Intensity–Potential Relations. Figure 4 shows the potential dependence of current and relative PL intensity recorded by sweeping the potential of the p-PS electrode at 20 mV/s between 0 and -1.2 V in 0.2 M Na_2SO_4 aqueous solution under excitation light wavelengths of 330, 360, and 390 nm. PL intensity was normalized to that at 0 V. The cathodic photocurrent due to hydrogen evolution increased, and the PL intensity decreased gradually when the potential became more negative than ca. -0.6 V. When the potential was swept back in the positive direction, the PL intensity increased and

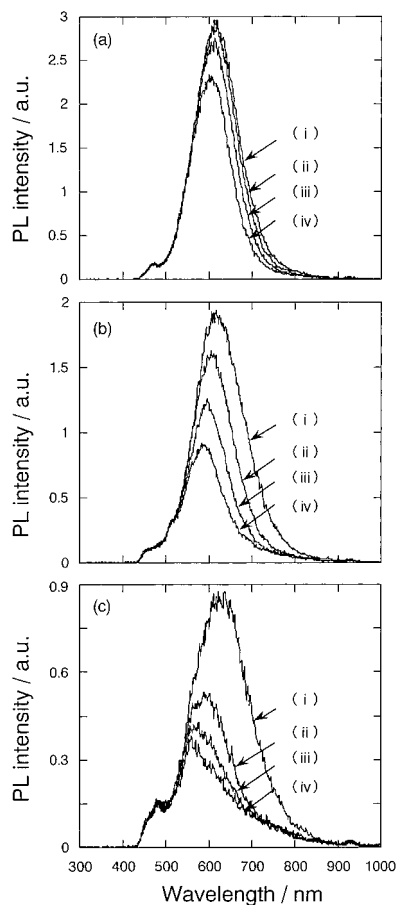


Figure 3. PL spectra observed at various negative potentials by sweeping the electrode potential with a sweep rate of 20 mV/s under monochromatic (a) 330, (b) 360, and (c) 390 nm excitation light. The spectra were measured at (i) -0.60 to -0.65 V, (ii) -1.05 to -1.10 V, (iii) -1.10 to -1.15 V, and (iv) -1.15 to -1.20 V.

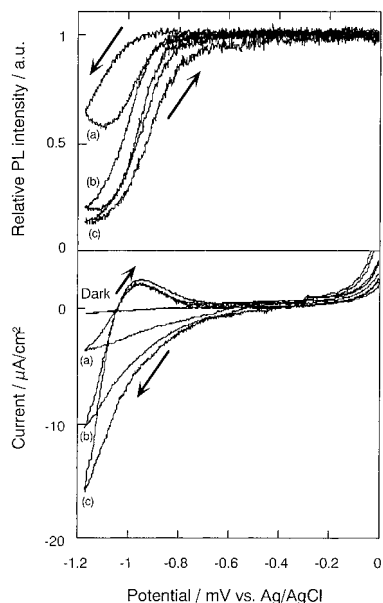


Figure 4. Potential dependence of PL intensity and cathodic photocurrent density with a sweep rate of 20 mV/s under monochromatic (a) 330, (b) 360, and (c) 390 nm excitation light. PL intensity (I) was normalized to that of the initial intensity (I_0).

returned to the initial intensity accompanied by a decrease of the cathodic photocurrent. The measurements using different excitation light wavelengths clearly showed that the larger photocurrent flowed and the PL was more quenched by longer wavelength excitation light. Note that this behavior of the

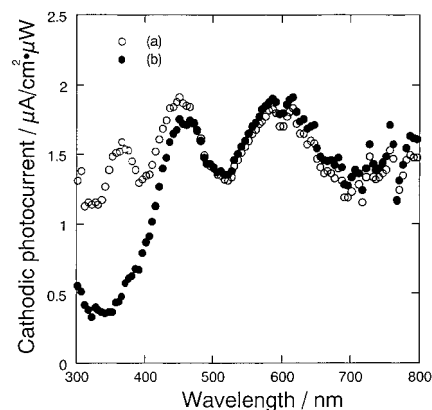


Figure 5. Cathodic photocurrent action spectra at the (a) p-Si and (b) p-PS electrodes in 0.2 M Na_2SO_4 at -1.2 V.

quenching coincides with that of the potential dependence of the PL spectra as shown in Figure 3.

Photocurrent Action Spectra at p-Type PS/Electrolyte Solution Interface. In order to discuss the origin of the photocurrent observed above, i.e., whether the cathodic photocurrent is arising from the Si substrate or from the PS layer, we measured the cathodic photocurrent action spectra of a p-Si and a p-PS electrodes at -1.2 V as shown in Figure 5. The cathodic photocurrent was normalized with respect to the light intensity to eliminate the effect of the excitation light intensity on cathodic photocurrent property. When the excitation wavelengths were longer than 500 nm, the response of the cathodic photocurrent was approximately the same for both p-Si and p-PS (ca. $1.5 \mu\text{A}/\text{cm}^2 \cdot \mu\text{W}$). When the excitation wavelengths became shorter than 500 nm, however, a decrease of the cathodic photocurrent was observed for the p-PS, although it was approximately constant for p-Si. The optical transmission spectra of PS measured by Koyama et al.¹⁸ using self-supporting p-PS layer, the PS layer is almost optically transparent in the wavelengths longer than 500 nm. Thus, it is possible to say that the decrease of the cathodic photocurrent observed in p-PS in the excitation light wavelength shorter than 500 nm observed in our experiments is due to the absorption of incident photons by PS layer formed on Si substrate which acts just like a short cut optical filter for Si substrate. Most of the incident photons in the wavelength shorter than 500 nm will contribute to the initial efficient PL as we observed in Figure 1. Only a few photons are able to reach the Si substrate and contribute to generate photocarriers. Hence, we concluded that the cathodic photocurrent observed during the potential scan in Figure 4 is arising from the Si substrate.

Interpretation of Potential and Excitation Light Wavelength Dependence of PL from p-Type PS/Electrolyte Solution Interface. Recent investigations of electrically induced quenching of the PL intensity at an n-PS electrode in forward bias by Bsiesy et al.¹² and Meulenkaamp et al.¹³ have shown that this quenching is related to the changes in potential. Very recently, Peter et al.¹⁹ have observed a voltage tuning of EL from p-PS/persulfate solution interface under reverse bias condition where electrons were generated in the substrate by illuminating from the rear of the Si wafer. They also measured the interfacial capacitance of the p-PS/electrolyte solution and concluded that the electrons accumulated in the PS layer could be able to generate EL via the reduction of persulfate and recombine with the injected hole.^{19,20} They proposed a mechanism of the PL quenching based on a nonradiative Auger recombination of the electron-hole pair or exciton.^{12,13,19} Since the theoretically calculated nonradiative Auger recombination lifetime is of the order of 10^{-9} s for spherical quantum-sized

Si crystallites²¹ and is much shorter than the lifetime of the luminescent excited state (ca. 10^{-5} s), the light emission will be completely quenched if an electron is presented in the excited state. They did not, however, discuss the relation between the degree of the PL quenching and amount of photocurrent, which is one of the most important parameters to characterize the PS/electrolyte solution interface.

The photocurrent action spectra of the p-Si and p-PS showed that most of the incident photons are absorbed in the PS layer when the wavelength is shorter than 400 nm. Since PL measurements were carried out in this wavelength region, we should consider the mechanism with this fact in mind. The remaining photons reach the Si substrate and generate electron-hole pairs. The photogenerated electrons may either be swept into the confined state in the PS layer or contribute to hydrogen evolution at Si/electrolyte solution interface, i.e., photocurrent, with the competition of recombination with holes. As the potential becomes more negative, the Fermi level scans across the conduction band levels of the Si nanocrystallites toward the smaller size (large band gap), which leads to a shift in the optical absorption edge to higher energies by accumulation of electrons in the PS layer injected from the Si substrate induced by the electric field in the Si substrate. Therefore, the quenching from the red portion (low energy) of the PL spectra is observed by increasing the negative potential (Figure 3). Note that our results are quite analogous with that seen in the previous works with n-PS/electrolyte solution interface under forward bias conditions.^{12,13}

The excitation wavelength dependence of the photocurrent and the PL quenching can be explained qualitatively by considering the optical penetration depth of the excitation light wavelength. Longer wavelength light will penetrate deeper in Si substrate and generate more photogenerated electrons. A large population of photogenerated electrons will lead to both high probability to enter the confined energy states in PS layer and large cathodic photocurrent at the Si/electrolyte solution interface. Hence, quenching of the lower energy portion of the PL spectra becomes faster and the cathodic photocurrent becomes larger in the case of longer excitation wavelength light than in the case of shorter one even at the same potential.

Conclusion

The photoelectrochemical and PL properties of the p-PS/electrolyte solution interface were investigated. It has been demonstrated that voltage tuning of the PL spectra is observed even at the p-PS/electrolyte solution interface under reverse bias region. A quenching of the PL intensity accompanied by a blue shift of the peak wavelength, as a result of the quenching of the red portion of the PL spectra, and increased photocurrent were observed by making the potential more negative. The longer the excitation light wavelength, the larger the observed quenching. The experimentally observed results can be explained by considering the dependence of electron accumulation on the conduction band levels in PS layer, which is in turn related to the Si nanocrystalline size.

Acknowledgment. This work was partially supported by Grants-in-Aids on Priority-Area-Research "Photoreaction Dynamics" from the Ministry of Education, Science, Sports and Culture, Japan (Nos. 06239204, 07228204, and 08218204). We

are grateful to Mr. Kitazawa of Shin-Etsu Semiconductor for the donation of Si wafers.

References and Notes

- (1) Canham, L. T. *Appl. Phys. Lett.* **1990**, *57*, 1046.
- (2) (a) Koshida, N.; Koyama, H. *Appl. Phys. Lett.* **1992**, *60*, 347. (b) Richter, A.; Lang, W.; Steiner, P.; Kozlowski, F.; Sandmaier, H. *Mater. Res. Soc.* **1992**, *256*, 209. (c) Namavar, F.; Marusaka, H. P.; Kalahoran, N. M. *Appl. Phys. Lett.* **1992**, *60*, 2514. (d) Futagi, T.; Matsumoto, T.; Katsuno, M.; Ohta, Y.; Mimura, H.; Kitamura, K. *Jpn. J. Appl. Phys.* **1992**, *31*, L616. (e) Hirschman, K. D.; Tsybeskov, L.; Duttagupta, S. P.; Fauchet, P. M. *Nature* **1996**, *384*, 338.
- (3) (a) Lehmann, V.; Gösele, U. *Appl. Phys. Lett.* **1991**, *58*, 856. (b) Sawada, S.; Hamada, N.; Ookubo, N. *Phys. Rev. B* **1994**, *49*, 5236. (c) Read, A. J.; Needs, R. J.; Nash, K. J.; Canham, L. T.; Calcott, P. D. J.; Qteish, A. *Phys. Rev. Lett.* **1992**, *69*, 1232. (d) Kanemitsu, Y.; Uto, H.; Masumoto, Y.; Futagi, T.; Mimura, H. *Phys. Rev. B* **1993**, *48*, 2827.
- (4) (a) Takagahara, T.; Takeda, K. *Phys. Rev. B* **1992**, *46*, 15578. (b) Lippens, P. E.; Lannoo, M. *Phys. Rev. B* **1989**, *39*, 1093.
- (5) (a) Brant, M. S.; Fuchs, H. D.; Stutzmann, M.; Weber, J.; Cardona, M. *Solid State Commun.* **1992**, *81*, 307. (b) Pokers, S. M.; Glembocki, O. J.; Bermudez, V. M.; Kaplan, R.; Friedersdorf, L. E.; Searson, P. C. *Phys. Rev. B* **1992**, *45*, 13788.
- (6) (a) Uosaki, K.; *Trends Anal. Chem.* **1990**, *9*, 98. (b) Petermann, G.; Tributsch, H.; Bogomolni, R. *J. Chem. Phys.* **1972**, *57*, 1026.
- (7) (a) Pettinger, B.; Schöppel, H.-R.; Yokoyama, T.; Gerischer, H. *Ber. Bunsenges. Phys. Chem.* **1974**, *78*, 1024. (b) Fan, F.-R. F.; Leempoel, P.; Bard, A. J. *J. Electrochem. Soc.* **1983**, *130*, 1866. (c) Uosaki, K.; Kita, H. *Bull. Chem. Soc. Jpn.* **1984**, *57*, 3247.
- (8) (a) Bresser, P. M. M. C.; Knapen, J. W. J.; Meulenkamp, E. A.; Kelly, J. J. *Appl. Phys. Lett.* **1992**, *61*, 108. (b) Canham, L. T.; Leong, W. Y.; Beale, M. I. J.; Cox, T. I.; Taylor, L. *Appl. Phys. Lett.* **1992**, *61*, 2563. (c) Bsiesy, A.; Muller, F.; Ligeon, M.; Gaspard, F.; Herino, R.; Romestain, R.; Vial, J. C. *Phys. Rev. Lett.* **1993**, *71*, 637. (d) Ogasawara, K.; Momma, T.; Osaka, T. *Chem. Lett.* **1994**, 1243. (e) Ogasawara, K.; Momma, T.; Osaka, T. *J. Electrochem. Soc.* **1995**, *142*, 1874. (f) Uosaki, K.; Noguchi, H.; Murakoshi, K.; Kondo, T. *Chem. Lett.* **1995**, 667. (g) Kooij, E. S.; Noordhoek, S. M.; Kelly, J. J. *J. Phys. Chem.* **1996**, *100*, 10754.
- (9) (a) Canham, L. T.; Leong, W. Y.; Beale, M. I. J.; Cox, T. I.; Taylor, L. *Appl. Phys. Lett.* **1992**, *61*, 2563. (b) Halimaoui, A.; Oules, C.; Bomchil, G.; Bsiesy, A.; Gaspard, F.; Herino, R.; Ligeon, M.; Muller, F. *Appl. Phys. Lett.* **1991**, *59*, 304. (c) Billat, S. *J. Electrochem. Soc.* **1996**, *143*, 1055. (d) Kooij, E. S.; Rama, A. R.; Kelly, J. J. *Surf. Sci.* **1997**, *370*, 125.
- (10) (a) Kondo, T.; Kim, Y. Y.; Uosaki, K. *Denki Kagaku* **1994**, *62*, 540. (b) Uosaki, K.; Kondo, T.; Noguchi, H.; Murakoshi, K.; Kim, Y. Y. *J. Phys. Chem.* **1996**, *100*, 4564.
- (11) Murakoshi, K.; Uosaki, K. *Appl. Phys. Lett.* **1993**, *62*, 1676.
- (12) (a) Bsiesy, A.; Muller, F.; Mihalcescu, I.; Ligeon, M.; Gaspard, F.; Herino, R.; Romestain, R.; Vial, J. C. *J. Lumin.* **1993**, *57*, 29. (b) Bsiesy, A.; Vial, J. C.; Gaspard, F.; Herino, R.; Ligeon, M.; Mihalcescu, I.; Muller, F.; Romestain, R. *J. Electrochem. Soc.* **1994**, *141*, 3071. (c) Mihalcescu, I.; Vial, J. C.; Bsiesy, A.; Muller, F.; Romestain, R.; Martin, E.; Delerue, C.; Lannoo, M.; Allen, G. *Phys. Rev. B* **1995**, *51*, 17605. (d) Hory, M. A.; Bsiesy, A.; Herino, R.; Ligeon, M.; Muller, F.; Vial, J. C. *Thin Solid Films* **1996**, *276*, 130.
- (13) (a) Meulenkamp, E. A.; Peter, L. M.; Riley, D. J.; Wielgosz, R. I. *J. Electroanal. Chem.* **1995**, *392*, 97. (b) Peter, L. M.; Riley, D. J.; Wielgosz, R. I.; Snow, P. A.; Penty, R. V.; White, I. H.; Meulenkamp, E. A. *Thin Solid Films* **1996**, *276*, 123.
- (14) (a) Petermann, G.; Tributsch, H.; Bogomolni, R. *J. Chem. Phys.* **1972**, *57*, 1026. (b) Karas, B. R.; Ellis, A. B. *J. Am. Chem. Soc.* **1980**, *102*, 968. (c) Kaneko, S.; Uosaki, K.; Kita, H. *J. Phys. Chem.* **1986**, *90*, 6654. (d) Uosaki, K.; Shigematsu, Y.; Kaneko, S.; Kita, H. *J. Phys. Chem.* **1989**, *93*, 6521.
- (15) Halimaoui, A. *Appl. Phys. Lett.* **1993**, *63*, 1264.
- (16) Canham, L. T.; Houlton, M. R.; Leong, W. Y.; Pickering, C.; Keen, J. M. *J. Appl. Phys.* **1991**, *70*, 422.
- (17) Arita, Y.; Sunohara, Y. *J. Electrochem. Soc.* **1977**, *124*, 285.
- (18) Koyama, H.; Araki, M.; Yamamoto, Y. *Jpn. J. Appl. Phys.* **1991**, *30*, 3606.
- (19) Peter, L. M.; Wielgosz, R. I. *Appl. Phys. Lett.* **1996**, *69*, 806.
- (20) (a) Peter, L. M.; Riley, D. J.; Wielgosz, R. I. *Appl. Phys. Lett.* **1995**, *66*, 2355. (b) Peter, L. M.; Riely, D. J.; Wielgosz, R. I. *Thin Solid Films* **1996**, *276*, 61.
- (21) Delerue, C.; Lannoo, M.; Allan, G.; Martin, E. *Thin Solid Films* **1995**, *255*, 27.